LETTERS
PUBLISHED ONLINE: 20 JULY 2015 | DOI: 10.1038/NCLIMATE2722
nature climate change

Impact of ocean acidification on the structure of future phytoplankton communities

Stephanie Dutkiewicz[1,2*], J. Jeffrey Morris[3,4†], Michael J. Follows[2], Jeffery Scott[1,2], Orly Levitan[5], Sonya T. Dyhrman[6] and Ilana Berman-Frank[7]

Phytoplankton form the foundation of the marine food web and regulate key biogeochemical processes. These organisms face multiple environmental changes[1], including the decline in ocean pH (ocean acidification) caused by rising atmospheric p_{CO_2} (ref. 2). A meta-analysis of published experimental data assessing growth rates of different phytoplankton taxa under both ambient and elevated p_{CO_2} conditions revealed a significant range of responses. This effect of ocean acidification was incorporated into a global marine ecosystem model to explore how marine phytoplankton communities might be impacted over the course of a hypothetical twenty-first century. Results emphasized that the differing responses to elevated p_{CO_2} caused sufficient changes in competitive fitness between phytoplankton types to significantly alter community structure. At the level of ecological function of the phytoplankton community, acidification had a greater impact than warming or reduced nutrient supply. The model suggested that longer timescales of competition- and transport-mediated adjustments are essential for predicting changes to phytoplankton community structure.

The world's oceans have absorbed about 30% of anthropogenic carbon emissions, causing a significant decrease in surface ocean pH (ref. 2). Concerns over the impacts of ocean acidification (OA) on marine life have led to a number of laboratory and field experiments examining the response of marine biota to acidification.

OA is not the only driver that is affecting marine ecosystems[1,3]. The oceans are warming, and nutrient and light environments are changing. Numerical models (for example, refs 4–6) have explored how these other drivers impact primary productivity, although less emphasis has been placed on changes in community structure. Phytoplankton types are not physiologically interchangeable, and the specific taxa in a community can impact the cycling of elements and the flow of nutrients and energy through the marine food web. In this study we employed a meta-analysis of OA experiments as input for a numerical model to explore how OA, relative to other drivers, may change phytoplankton community composition.

We compiled data from 49 papers (Methods and Supplementary Table 1) in which direct comparisons were made between the growth rates of marine phytoplankton cultures exposed to ambient p_{CO_2} (~380 μatm) versus elevated p_{CO_2} within the range predicted by 2100 (refs 2,7; ~700–1,000 μatm). The tested organisms were split into six groups: two picocyanobacteria (*Prochlorococcus* and *Synechococcus*); nitrogen-fixing cyanobacteria (diazotrophs); and three larger eukaryotic groups (diatoms, coccolithophores, and other large taxa such as dinoflagellates). Given the different roles these groups play in nutrient cycling we refer to them as 'functional groups'. For example, diatoms require silica, diazotrophs add fixed nitrogen to the environment, and picophytoplankton harvest nutrients more efficiently than other groups.

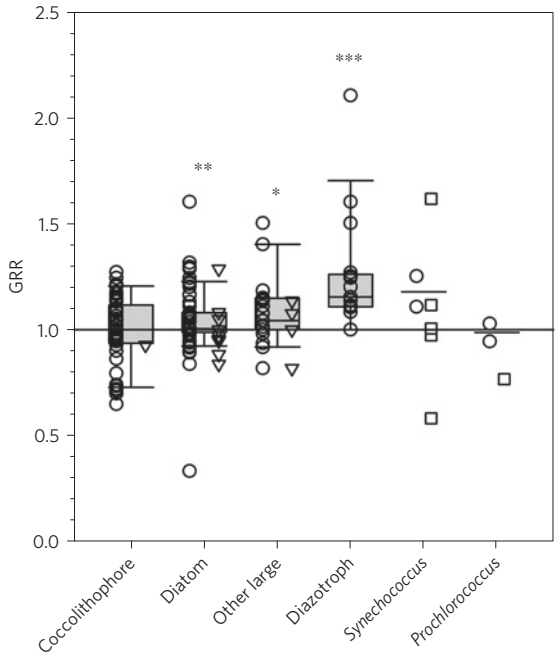

Figure 1 | Meta-analysis of GRR of phytoplankton in p_{CO_2} manipulation experiments. Circles represent observations comparing laboratory cultures at high and ambient p_{CO_2}; triangles indicate long-term experiments; squares represent data from mixed community field incubations. Grey boxes span the 25th–75th percentiles; central lines indicate median values; whiskers extend from the 10th to the 90th percentiles. Significance values are based on Wilcoxon signed-rank tests against the value of 1. *, $p < 0.05$; **, $p < 0.01$; ***, $p < 0.001$.

[1]Center for Global Change Science, Massachusetts Institute of Technology, Cambridge, Massachusetts 02139, USA. [2]Earth, Atmospheric and Planetary Sciences, Massachusetts Institute of Technology, Cambridge, Massachusetts 02139, USA. [3]Department of Microbiology and Molecular Genetics, Michigan State University, East Lansing, Michigan 48824, USA. [4]BEACON Center for the Study of Evolution in Action, Michigan State University, East Lansing, Michigan 48824, USA. [5]Environmental Biophysics and Molecular Ecology Program, Institute of Marine and Coastal Sciences, Rutgers University, New Brunswick, New Jersey 08901, USA. [6]Department of Earth and Environmental Sciences and the Lamont-Doherty Earth Observatory, Colombia University, Palisades, New York 10964, USA. [7]Mina and Everard Goodman Faculty of Life Sciences, Bar-Ilan University, Ramat Gan 52900, Israel. †Present address: Department of Biology, University of Alabama at Birmingham, Birmingham, Alabama 35294, USA. *e-mail: stephd@mit.edu

Table 1 | Summary of GRR to elevated p_{CO_2} for six phytoplankton functional groups.

Functional group	GRR	Minimum	Maximum	N_{obs}	N_{spp}	$N_{strains}$
Coccolithophores	1.001 ± 0.155	0.648	1.269	45	4	17
Diatoms	1.042 ± 0.150	0.333	1.600	68	22	22
Other large	1.093 ± 0.172	0.818	1.5	20	12	12
Diazotrophs	1.248 ± 0.269	1.000	2.102	17	3	4
Synechococcus	1.179 ± 0.101	0.944	1.029	2	1	1
Prochlorococcus	0.987 ± 0.059	1.108	1.250	2	1	1

GRR values are means ± s.d. N_{obs}, N_{spp} and $N_{strains}$ are the numbers of total observations, different species and different strains, respectively.

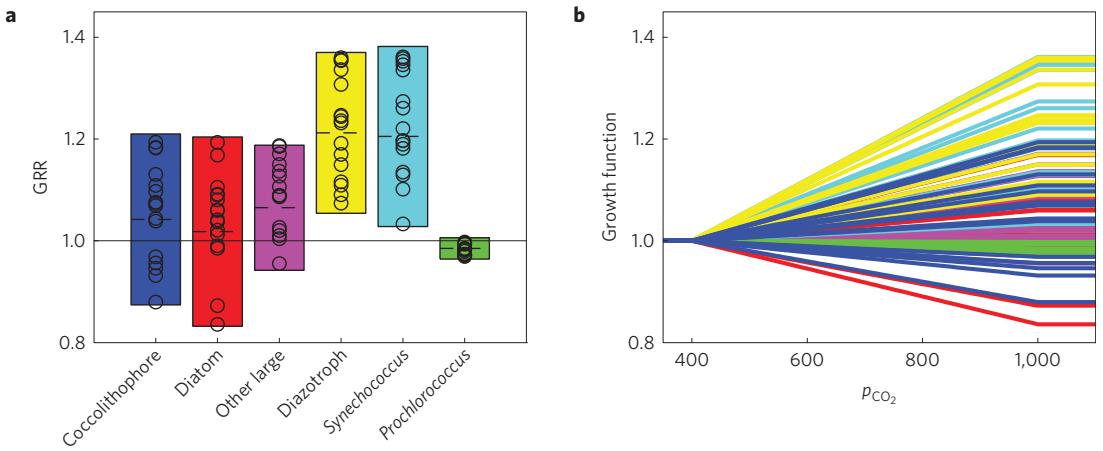

Figure 2 | Model parameterization of GRR to elevated p_{CO_2}. a, Solid bars indicates mean ± 1 s.d. of normalized GRR to elevated p_{CO_2} from the single species meta-analysis (Table 1). Circles indicate stochastically chosen GRR for 16 types within each functional group (for one ensemble member). GRR of 1.2 = 20% increase in growth rate. **b**, Model parameterization of growth function with increasing p_{CO_2}; colours indicate the functional groups as shown in **a**. The function is unitless: actual growth rates depended also on the maximum growth rate specific for each functional group, as well as nutrient, light and temperature.

We calculated the growth rate response (GRR) of each of the 154 observations in our meta-analysis as the ratio of growth rates under elevated versus ambient p_{CO_2} (Table 1). Values greater than one indicate faster growth at higher p_{CO_2}. There was a wide range of responses between taxa, within functional groups (Fig. 1), and even differing responses between strains of the same species[8,9]. The median GRRs of diazotrophs as well as all eukaryotes (except coccolithophores) were statistically greater than one (Wilcoxon signed-rank tests, $p < 0.05$). There were too few observations of picocyanobacteria for statistical analysis, but the two *Synechococcus* data points fell within the range of the diazotrophic cyanobacteria, whereas *Prochlorococcus* appeared to be nearly unaffected by elevated p_{CO_2} (ref. 10). For some eukaryotic phytoplankton[11–14] GRRs could also be computed both before and after long-term cultivation at elevated p_{CO_2} (for example, long enough for evolutionary changes). Although changes in culture growth rates were observed in these experiments, GRRs remained within the range shown by other culture studies (Fig. 1, triangles). GRRs from our re-analysis of a set of shipboard incubation experiments[15] are also included (Fig. 1, squares and Supplementary Table 2).

Not only was there a wide range within functional groups, but GRRs also differed significantly between the functional groups (Kruskal–Wallis test, $df = 5$, $\chi^2 = 21.8$, $p < 0.001$), suggesting that changes in p_{CO_2} may impact competition both within and between groups. To test this possibility we employed a marine ecosystem model[5] that incorporated the six functional groups embedded in the ocean component of an earth system model[16]. Within each functional group 16 'types' with differing temperature ranges and growth optima[17–19] were resolved (Supplementary Fig. 1a). Each of the 96 types was also assigned a random p_{CO_2} GRR within the range (mean ± 1 s.d.) suggested by the meta-analysis for each functional group (Fig. 2).

We simulated the perturbation of the model marine ecosystem from pre-industrial conditions through 2100 under a 'business as usual' scenario[16] similar to IPCC Representative Concentration Pathway (RCP)8.5 (ref. 7). The biogeochemistry, productivity and community structure in the simulated present-day ocean (Supplementary Figs 3–5) were consistent with observations, with oligotrophic waters dominated by picophytoplankton and regions of higher nutrient supply dominated by eukaryotes. We note that the modelled range of *Synechococcus* included that observed for pico-eukaryotes that are not resolved in this model.

The model ocean changes through the twenty-first century included warming waters, decreased macronutrient supply, altered light environments, increased p_{CO_2} and lower pH (Supplementary Fig. 6). By 2100, temperatures and nutrient conditions were shifted latitudinally relative to 2000, but p_{CO_2} was substantially altered everywhere in the open ocean (Supplementary Fig. 7, although in the real ocean localized coastal regions can at present reach such higher values[20]). We focused on global changes to phytoplankton community structure and biogeography as a result of these physicochemical alterations (Figs 3 and 4 and Supplementary Figs 4b and 8). In general, types with GRR < 1 had reduced biomass by the end of the century (Fig. 3a). However, the 'losers' in the future world were not only the types with GRR < 1; many types that had enhanced growth with higher p_{CO_2} were nevertheless outcompeted. The largest gains in biomass (relative to present day) were from types with the highest GRR, typically *Synechococcus* and diazotrophs, yet

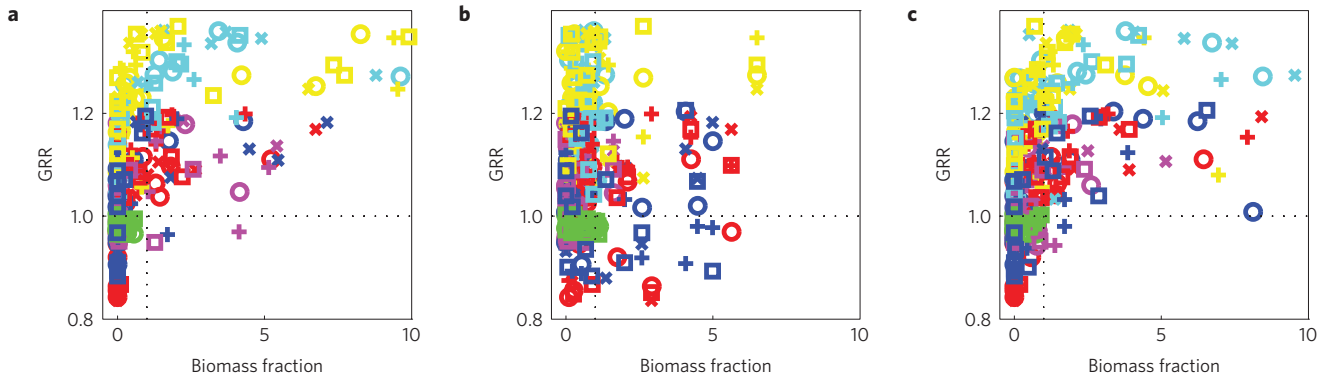

Figure 3 | Biomass change between 2000 and 2100. a–c, Fraction of globally integrated biomass of each of the 96 phytoplankton types at 2100 relative to 2000 as a function of GRR for experiments ALL, with all drivers (**a**); ALL-OTHER (other drivers, but no p_{CO_2} changes) (**b**); p_{CO_2}-ONLY (**c**). Colours indicate the different functional groups (see Fig. 2) and different symbols represent each of the four ensemble members. Symbols to left of vertical line (biomass fraction = 1) indicates reduction in biomass relative to present day. Also indicated is GRR = 1; for **a**,**c**, symbols above this line indicate types that had a higher growth rate with enhanced p_{CO_2}. In **b**, p_{CO_2} does not change, but types are plotted in the same way for illustrative purposes.

even some types in these two functional groups had substantial decreases in biomass.

As a metric of community structure we define the 'functional diversity' as the local assemblage of the summed members of the six functional groups. We quantified this metric as the proportion of the pre-industrial community that remained at any location[5] (see Methods). A value <1 indicates a change in community, although not necessarily with decreased biomass or diversity, as a new community could have invaded (Supplementary Fig. 9), as has been observed in the real ocean[21]. Changes were calculated at each location and averaged globally. Global functional diversity was altered by ~50% (Fig. 4a), with broad-scale changes in dominant functional groups relative to pre-industrial conditions (Supplementary Fig. 4b). The mean range of the 96 phytoplankton types shifted polewards by almost 600 km by year 2100 (Fig. 4b). Although there was little change in globally integrated primary production (Fig. 4c), there were substantial regional changes (Supplementary Fig. 10), depending on whether light/temperature or nutrients was limiting growth[5,6]. Model results appeared robust across an ensemble of four replicate simulations, each with a different array of randomized GRRs.

To explore how acidification relative to other global change drivers contributed to these responses, two additional simulations were conducted (details in Methods). In one simulation, experiment p_{CO_2}-ONLY, p_{CO_2} was allowed to rise while all other fields remained as for pre-industrial conditions. In the other, experiment ALL-OTHERS, p_{CO_2} was held at pre-industrial conditions while all other fields impacting growth were allowed to change.

In ALL-OTHERS, which captures the drivers that previous models[4–6] have included, phytoplankton biomass was not influenced by GRR (Fig. 3b), but instead was determined by alterations in temperature, nutrient availability (Supplementary Fig. 7a,b) and irradiance. Habitat ranges of phytoplankton types moved polewards at the same rate as the temperature fields (Fig. 4b) with some polar species becoming extinct[5]. The increasingly oligotrophic conditions[5,22] favoured picophytoplankton, leading to a modest change in functional diversity (Fig. 4a). However, the dominant functional groups in most regions remained largely reminiscent of pre-industrial conditions (Supplementary Fig. 4c), although these groups were composed of types with different (warmer) temperature optima which significantly altered the genetic profile in 2100 (ref. 5) (Fig. 3b and Supplementary Fig. 11b). Reduced nutrient supply led to a 5% decrease in globally integrated primary production[4,5,22] (Fig. 4c).

In the model experiment p_{CO_2}-ONLY there was instead an increase in globally integrated primary production (Fig. 4c) due to

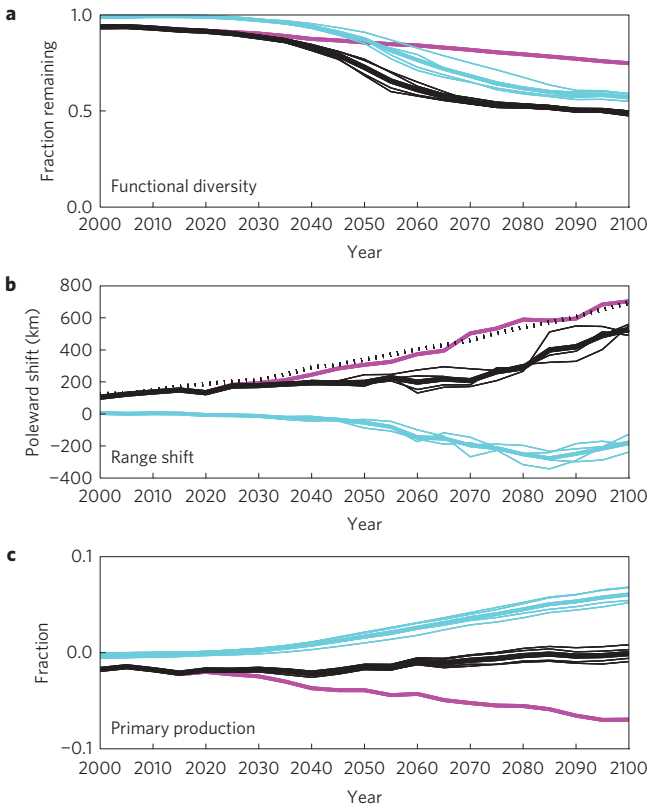

Figure 4 | Modelled global changes over the twenty-first century. a, Global mean fraction of functional group community (functional diversity) remaining at each location. **b**, Mean latitudinal poleward shift of leading edge of the 96 phytoplankton types' habitats. **c**, Fractional change in globally integrated primary production. Purple indicates experiment ALL-OTHER; blue indicates p_{CO_2}-ONLY; black indicates ALL. For ALL and p_{CO_2}-ONLY, thin lines are the ensemble members and thick line is the ensemble mean. Dotted black line in **b** indicates the mean shift in isotherms.

the higher mean growth rate with elevated p_{CO_2} (the mean GRR over all observations was 1.06). In agreement with field manipulation experiments[23–27], primary production increased in high-nutrient regions and remained relatively constant in oligotrophic regions under ambient nutrient conditions (Supplementary Fig. 10c). The

fractional increase in globally integrated primary production in the full model (experiment ALL) resulted from the compensating effect of one enhancing driver (p_{CO_2}) and one restrictive driver (reduced nutrients).

In p_{CO_2}-ONLY there were substantial alterations in phytoplankton types' biomass by 2100 (Fig. 3c and Supplementary Fig. 4b). Here, differences in GRRs alone caused these changes and yet many with GRR > 1 declined. Even slightly higher GRR relative to a competitor would allow one phytoplankton to outcompete another. Field studies measuring changes in functional group abundance during p_{CO_2} manipulations have shown that changing p_{CO_2} alone can have pronounced impacts on community structure[23–27].

The response in the full model (ALL, Fig. 3a) was a combination of the different drivers (Fig. 3b,c). However, OA was the greatest driver of changes in biomass (Fig. 3) and functional diversity (Fig. 4a) by mid-century, although the exact timing was sensitive to the parameterization of growth to elevated p_{CO_2} (see sensitivity studies, Supplementary Figs 2 and 12). As some types were regionally outcompeted, their range decreased, manifesting in an equatorward shift in the mean ranges (as seen for p_{CO_2}-ONLY, Fig. 4b). Thus, when considering experiment ALL we found that the mean habitat change no longer followed the temperature predictions seen in ALL-OTHERS and often assumed[18,28].

In our model (and the real ocean[17,18]) the distribution of temperature tolerances was similar between functional groups, and therefore functional diversity was largely preserved in ALL-OTHERS, with individual types tracking their optimal temperatures polewards (Fig. 4b and Supplementary Fig. 7a). In contrast, the distribution of p_{CO_2} GRRs was significantly different amongst types and functional groups (Fig. 1). Moreover present-day variations in open ocean p_{CO_2} do not overlap those projected for 2100 (Supplementary Fig. 7c). This suggests why OA, rather than temperature, was ultimately a stronger driver of functional diversity changes in our model—a finding that contradicts several field experiments[12,27] that manipulated temperature and p_{CO_2}. We acknowledge that field experiments are crucial for providing benchmarks to understand complex community response under climate change. However, we suggest that such experiments with the relatively sudden effects of temperature stress and lack of transport in of new species may mask the more subtle influence of OA on competition, which may require many generations to produce major effects.

Our study highlights the need for experiments designed to map phytoplankton growth responses over a full range of p_{CO_2} and the need for a better understanding of the physiological trade-offs governing adaptation of phototrophs to a high-p_{CO_2} world. A number of recent studies of long-term evolutionary responses to OA and other climate change drivers[11–14,29], as well as studies investigating synergisms between OA, temperature and other metabolic and environmental stressors[3,30], are beginning to address these questions. Future models will need to incorporate their findings to make more realistic predictions about the fate of phytoplankton communities in an acidifying ocean.

Our model results, guided by a synthesis of disparate laboratory studies, indicate that p_{CO_2}-related differences in competitive fitness are of sufficient magnitude to considerably alter phytoplankton community function over the coming decades. Given the importance of competition shown here, detailed experimental observations of inter- and intra-group competitive interactions will be essential for advancing our ability to predict future community shifts. The effect of long timescales and the role of transport are important determinants of changes in phytoplankton community structure and highlight the importance of modelling alongside laboratory and field experiments. Such multi-pronged research is critical as the large turnover of community functionality suggested by our model could carry profound consequences for all levels of the marine food chain, as well as global biogeochemistry.

Methods

Methods and any associated references are available in the online version of the paper.

Received 20 January 2015; accepted 12 June 2015; published online 20 July 2015

References

1. Gruber, N. Warming up, turning sour, losing breath: Ocean biogeochemistry under global change. *Phil. Trans. R. Soc. A* **369,** 1980–1996 (2011).
2. Doney, S. C., Fabry, V. J., Feely, R. A. & Kleypas, J. A. Ocean acidification: The other CO_2 problem. *Annu. Rev. Mar. Sci.* **1,** 169–192 (2009).
3. Boyd, P. W. Framing biological responses to a changing ocean. *Nature Clim. Change* **3,** 530–533 (2013).
4. Bopp, L. *et al.* Multiple stressors of ocean ecosystems in the 21st century: Projections with CMIP5 models. *Biogeosciences* **10,** 6225–6245 (2013).
5. Dutkiewicz, S., Scott, J. R. & Follows, M. J. Winners and losers: Ecological and biogeochemical changes in a warming ocean. *Glob. Biogeochem. Cycles* **27,** 463–477 (2013).
6. Taucher, J. & Oschlies, A. Can we predict the direction of marine primary production change under global warming? *Geophys. Res. Lett.* **38,** LO2603 (2011).
7. IPCC *Climate Change 2013: The Physical Science Basis* (eds Stoker, T. F. *et al.*) (Cambridge Univ. Press, 2013).
8. Hutchins, D. A., Fu, F.-X., Webb, E. A., Walworth, N. & Tagliabue, A. Taxon-specific response of marine nitrogen fixers to elevated carbon dioxide concentrations. *Nature Geosci.* **6,** 790–795 (2013).
9. Langer, G., Nehrke, G., Probert, I., Ly, J. & Ziveri, P. Strain-specific responses of *Emiliania huxleyi* to changing seawater carbonate chemistry. *Biogeosciences* **6,** 2637–2646 (2009).
10. Fu, F. X., Warner, M. E., Zhang, Y. H., Feng, Y. Y. & Hutchins, D. A. Effects of increased temperature and CO_2 on photosynthesis, growth, and elemental ratios in marine *Synechococcus* and *Prochlorococcus* (Cyanobacteria). *J. Phycol.* **43,** 485–496 (2007).
11. Lohbeck, K. T. *et al.* Adaptive evolution of a key phytoplankton species to ocean acidification. *Nature Geosci.* **5,** 346–351 (2012).
12. Tatters, A. O. *et al.* Short- and long-term conditioning of a temperate marine diatom community to acidification and warming. *Phil. Trans. R. Soc. B* **368,** 20120437 (2013).
13. Crawfurd, K. J., Raven, J. A., Wheeler, G. L., Baxter, E. J. & Joint, I. The response of *Thalassiosira pseudonana* to long-term exposure to increased CO_2 and decreased pH. *PLoS ONE* **6,** e26695 (2011).
14. Tatters, A. O. *et al.* Short- versus long-term responses to changing CO_2 in a coastal dinoflagellate bloom: Implications for interspecific competitive interactions and community structure. *Evolution* **67,** 1879–1891 (2013).
15. Lomas, M. W. *et al.* Effect of ocean acidification on cyanobacteria in the subtropical North Atlantic. *Aquat. Microb. Ecol.* **66,** 211–222 (2012).
16. Sokolov, A. *et al.* Probabilistic forecast for 21st century climate based on uncertainties in emissions (without policy) and climate parameters. *J. Clim.* **22,** 5175–5204 (2009).
17. Boyd, P. W. *et al.* Marine phytoplankton temperature versus growth responses from polar to tropical waters—outcome of a scientific community-wide study. *PLoS ONE* **8,** e63091 (2013).
18. Thomas, M. K., Kremer, C. T., Klausmeier, C. A. & Litchman, E. A global pattern of thermal adaptation in marine phytoplankton. *Science* **338,** 1085–1088 (2012).
19. Eppley, R. W. Temperature and phytoplankton growth in the sea. *Fishery Bull.* **70,** 1063–1085 (1972).
20. Hofmann, G. E., Smith, J. E. & Johnson, K. S. High-frequency dynamics of ocean pH: A multi ecosystem comparison. *PLoS ONE* **6,** e28983 (2011).
21. Dornelas, M. *et al.* Assemblage time series reveal biodiversity change but not systematic loss. *Science* **344,** 296–299 (2014).
22. Bopp, L., Aumont, O., Cadule, P., Alvain, S. & Gehlen, M. Response of diatoms distribution to global warming and potential implications: A global model study. *Geophys. Res. Lett.* **32,** L19606 (2005).
23. Feng, Y. *et al.* Effects of increasing p_{CO_2} and temperature on the North Atlantic spring bloom. I. The phytoplankton community and biogeochemical response. *Mar. Ecol. Prog. Ser.* **288,** 13–25 (2009).
24. Kim, J.-M. *et al.* The effect of seawater CO_2 concentration on growth of a natural phytoplankton assemblage in a controlled mesocosm experiment. *Limnol. Oceanogr.* **51,** 1629–1636 (2006).
25. Brussaard, C. P. D. *et al.* Arctic microbial community dynamics influenced by elevated CO_2 levels. *Biogeosciences* **10,** 719–731 (2013).

26. Tortell, P. D., DiTullio, G. R., Sigman, D. M. & Morel, F. M. M. CO_2 effects on taxonomic composition and nutrient utilization in an Equatorial Pacific phytoplankton assemblage. *Mar. Ecol. Prog. Ser.* **236,** 37–43 (2002).
27. Hare, C. E. *et al.* Consequences of increased temperature and CO_2 for phytoplankton community structure in the Bering Sea. *Mar. Ecol. Prog. Ser.* **352,** 9–16 (2007).
28. Poloczanska, E. S. *et al.* Global imprint of climate change on marine life. *Nature Clim. Change* **3,** 919–925 (2013).
29. Schaum, E., Rost, B., Millar, A. J. & Collins, S. Variation in plastic responses of a globally distributed picoplankton species to ocean acidification. *Nature Clim. Change* **3,** 298–302 (2013).
30. Boyd, P. W., Lennartz, S. T., Glover, D. M. & Doney, S. C. Biological ramifications of climate-change-mediated oceanic multi-stressors. *Nature Clim. Change* **5,** 71–79 (2015).

Acknowledgements

We acknowledge funding from NSF grant OCE-1315201 (J.J.M., S.D., M.J.F., S.T.D.), DOE grant DE-FG02-94ER61937 (S.D., J.S.), the Gordon and Betty Moore foundation (S.D., M.J.F.), NSF grant OCE 13-14336 (S.T.D.), German–Israel Joint Research BMBF-MOST grant GR1950 (I.B.-F.), the BEACON Center for the Study of Evolution in Action NSF grant DBI-0939454 (J.J.M.) and a NASA Astrobiology Institute Postdoctoral Fellowship (J.J.M.).

Author contributions

S.D., M.J.F., J.J.M. and I.B.-F. conceived the experimental design, J.J.M. conducted the literature meta-analysis, J.S. provided the fields from the earth system model, S.D. conducted the numerical experiments and analysed the results. O.L., I.B.-F. and S.T.D. provided contextual input. S.D. and J.J.M. co-wrote the paper, with input from all authors, especially I.B.-F. and S.T.D.

Additional information

Supplementary information is available in the online version of the paper. Reprints and permissions information is available online at www.nature.com/reprints. Meta-analysis output is available on BCO-DMO site http://www.bco-dmo.org/dataset/554221. Correspondence and requests for materials should be addressed to S.D.

Competing financial interests

The authors declare no competing financial interests.

Methods

Compilation of acidification experiments. A search of the Web of Science was conducted using the phrase '(coccolith* OR diatom* OR prochloroc* OR synechoc* OR trichodes* OR crocosphae* OR diazotroph*) AND (CO_2 or 'carbon dioxide' OR 'ocean acidification') AND ('growth rate')'. Each paper that mentioned a comparison between ambient and elevated CO_2 conditions in the abstract was downloaded. Additional papers were selected based on reference lists from the above papers and personal communications with researchers. We further curated these papers by excluding any (Supplementary Table 3) that: did not actually compare growth rates at different CO_2 concentrations; did not specify the CO_2 levels examined; used CO_2 concentrations outside the range 250–1,100 µatm; attempted to separately manipulate CO_2 concentration and pH using organic buffers; manipulated CO_2/pH in such a way as to radically change alkalinity; presented data in such a way that it was impossible to calculate a ratio of elevated:ambient growth rates; included only freshwater species; or had been retracted. Results were divided into single species short-term laboratory studies, long-term (evolutionary) laboratory studies, and field experiments with mixed communities (Fig. 1). Values were collected from tabulated data in papers where possible; otherwise values were estimated visually from figures. No attempt was made to extract information about replication level, variance, or significance level of data; only experimental means were collected. Many papers examined the response to CO_2 enrichment under a variety of environmental conditions (for example, different light or nutrient levels). In this study, each environment was considered as a unique experiment, and no attempt was made to examine covariance or synergy between any other parameter and response to CO_2. Such synergy is probably important, but as yet there is too little data to make these distinctions.

To compare laboratory studies to field studies, we considered a number of field CO_2-enrichment experiments. Unfortunately, only one of these papers, Lomas *et al.*[15], provided sufficient data to allow calculation of GRR for specific functional groups. Supplementary Table 2 summarizes our re-analysis of the data set in Table 3 of Lomas and colleagues[15]. In four out of five paired experiments, *Prochlorococcus* cell density decreased during multi-day incubations at elevated p_{CO_2}. We note that growth rate reponses to elevated p_{CO_2} (GRR) values are meaningless when the test organism's numbers do not increase under one or both CO_2 treatments, and represent this case with no number in Supplementary Table 2. In contrast, *Synechococcus* cell density always increased, with GRR >1 in three out of five experiments. We note that the authors of the original paper[15] concluded, owing to the large variability and apparent contradictions between their treatments, that there were 'small or nonsignificant effects of pH' on the two genera. However, we nevertheless include these data in Fig. 1 for three reasons: the overall lack of relevant field observations in our meta-analysis; the overall lack of observations of *Synechococcus* and *Prochlorococcus* responses to elevated p_{CO_2}; and the fact that none of our other data points from the meta-analysis considered either the authors' intent or the statistical significance of their conclusions. Our study shows that any change, even small, can be important, especially relative to competitors (see Fig. 3). We suggest that further experiments are needed on the competition between these two species at elevated p_{CO_2}.

Finally, we considered a number of evolution experiments with phytoplankton cultures[11–14] to determine whether long-term adaptation to elevated p_{CO_2} could push strains outside of the range observed in short-term studies. We considered only experiments where single strains of marine phytoplankton belonging to one of the six functional groups considered in our simulation were adapted to high p_{CO_2} for at least 100 generations.

The full data set compiled from our meta-analysis, including many more observations than the growth rates reported here, is available for download via BCO-DMO: http://www.bco-dmo.org/dataset/554221.

Climate model. The MIT Integrated Global Systems Model (IGSM) framework[5,16] was used in this study. In this earth system model of intermediate complexity, the three-dimensional ocean circulation[31] had a horizontal resolution of 2° × 2.5° and 22 vertical levels ranging from 10 m in the surface to 500 m at depth. Ocean boundary layer physics and the effects of mesoscale eddies not captured at this coarse resolution are parameterized[32,33]. The ocean is coupled to a two-dimensional (latitude and height) atmospheric physical[34] and chemical module, and a terrestrial component[35] with hydrology[36], vegetation[37] and natural emissions[38]. The coupled system was spun up for 2000 years (using 1860 conditions) before simulating 1860 to 2100 changes. Atmospheric greenhouse gas and volcanic observations were specified from 1860 to 2000; for the twenty-first century, human emissions for a 'business as usual' scenario were predicted from an economics module[16] (similar to the IPCC AR5 RCP8.5 scenario[7]). In both the spin-up, historical and future simulation phases, the three-dimensional ocean was forced with prescribed wind fields. These fields had variability as provided by NCEP (ref. 39) re-analysis (de-trended winds over the period 1948 to 2007 were employed; these winds were 'recycled' for years outside this period), which produced interannual variability in the ocean model. An El Niño Southern Oscillation (ENSO)-type signal was apparent. For simplicity, we did not allow changes to the wind patterns and intensity in the future period. Although some clear patterns of changes in wind stress emerged from analysis of the archived results from coupled runs[40], considerable model uncertainty remained[41,42]. This aspect of physical changes to the system is beyond the scope of this work.

Ecosystem model. The ocean physical fields (velocities, mixing and temperature) from the climate model were used to drive a modified version of the marine ecosystem model[5]. Inorganic and organic forms of carbon, nitrogen, phosphorus, iron and silica, as well as 96 phytoplankton types and two grazers were transported in the three-dimensional ocean. The biogeochemical and biological tracers interacted through the formation, transformation and remineralization of organic matter. Iron chemistry included explicit complexation with an organic ligand, scavenging by particles[43] and representation of aeolian[44] and sedimentary[45] sources.

Phytoplankton growth rates were parameterized as functions of the maximum photosynthesis rate, local light, nutrients temperature, as in previous studies[5], as well as p_{CO_2}.

Nutrient limitation of growth was determined by the most limiting resource,

$$\gamma_j^N = \min\left(N_1^{\lim}, N_2^{\lim}, \ldots\right)$$

where the nutrients (N_i) considered were phosphate, iron, silicic acid and dissolved inorganic nitrogen, and j represents phytoplankton type j ($j=1$–96). The effect on growth rate of ambient phosphate, iron or silicic acid concentrations was represented by a Michaelis–Menten function:

$$N_i^{\lim} = \frac{N_i}{N_i + k_{ij}}$$

where the k_{ij} were half-saturation constants for phytoplankton type j with respect to the ambient concentration of nutrient i. We resolved three potential sources of inorganic nitrogen (ammonia, nitrite and nitrate). Phytoplankton preferentially used ammonia.

Each functional group had different values of maximum photosynthesis rate, nutrient half-saturation constant, and potentially had different nutrient needs, as in our previous studies[5,46,47]. For instance, diatoms were parameterized to have the highest maximum photosynthesis, but also a high nutrient half-saturation and silicate requirements. *Prochlorococcus* had the lowest growth rate, but also the lowest half-saturation. These differences allowed each functional group to have a distinct and plausible spatial and temporal niche within our model[5,46,47] (Supplementary Fig. 4).

Temperature modulation of growth was represented by a non-dimensional factor (Supplementary Fig. 1a). This factor[48] was a function of ambient temperature, $T(K)$:

$$\gamma_j^T = \tau_T \exp\left(A_T\left(\frac{1}{T} - \frac{1}{T_N}\right)\right)\exp(-B_T|T - T_{oj}|^b) \quad (1)$$

Coefficient τ_T normalized the maximum value, whereas A_T, B_T, T_N and b regulated the sensitivity envelope. T_{oj} sets the optimum temperature specific to each of the 16 types in each functional group. There was an increase in maximum growth rate for types with higher optimum temperature, as suggested by observations[19,49], and a specific temperature range over which each type could grow, as suggested by observations[17,18]. We test other assumptions on the temperature growth function (Supplementary Figs 1b,c and 13; discussed later).

The unique feature of this model was the inclusion of a modification to growth rate by the ambient p_{CO_2} (Fig. 2 and Supplementary Fig. 2a):

$$\begin{aligned}
\gamma_j^{pCO_2} &= 1 \quad \text{if } p_{CO_2} < 400 \\
\gamma_j^{pCO_2} &= 1 + \delta_j \frac{(p_{CO_2} - 400)}{600} \quad \text{if } 400 < p_{CO_2} < 1{,}000 \\
\gamma_j^{pCO_2} &= 1 + \delta_j \quad \text{if } p_{CO_2} > 1{,}000
\end{aligned} \quad (2)$$

where δ_j was a randomly assigned coefficient from the range of responses seen in each functional group from the meta-analysis (that is, GRR, Fig. 1, Table 1). If $\delta_j = 0$, then there was no change in growth rate with increased p_{CO_2}, if $\delta_j = 0.2$ then the phytoplankton grew 20% faster when p_{CO_2} reached 1,000 µatm.

Because the meta-analysis focused on elevated p_{CO_2} and not the effects of pre-industrial low p_{CO_2}, we assumed that p_{CO_2} had no effect on growth rate until 400 µatm, and that there was a linear change from 400 to 1,000 µatm (Fig. 2). This simplest linear description was chosen as the majority of laboratory experiments conducted only present day and 'elevated' p_{CO_2}. Experiments conducted over a wider range of p_{CO_2} values suggested a hyperbolic Michaelis–Menten response for nitrogen fixation rates for *Trichodesmium* and *Crocosphaera*[8], but the GRR in that study (and others) appeared more complex. We do test how more complex p_{CO_2}

growth functions (Supplementary Fig. 2b,c) alter the results (Supplementary Section 4, Supplementary Fig. 12,) finding that the function does affect the speed of response, but not the final 2100 results.

Furthermore, many studies factorially (for example, many in Supplementary Table 1) manipulated p_{CO_2} in addition to other environmental parameters, such as temperature and nutrient concentration. Often these experiments suggested some form of synergy between CO_2 and other factors, but there was no cross-system consensus as to how any of these factors interacted.

Primary production was calculated as a function of photosynthesis rate (a function of nutrients, light, p_{CO_2} and temperature) and phytoplankton biomass (B_j) summed across all phytoplankton types ($j=1$–96).

Simulation design. Nutrient distributions were initialized from results from previous simulations, although the results presented here were not sensitive to these initial conditions. The 96 phytoplankton types were all initialized with the same low initial condition. The ecosystem was forced with the physical fields from the earth system model for the pre-industrial control and run for 50 years to allow the phytoplankton community and the upper ocean biogeochemistry to establish a quasi-equilibrium. A repeating seasonal cycle was quickly reached and there was only a small biogeochemical drift associated with upwelling of deep water. The several thousand years of integration needed to adjust the deep ocean was computationally unfeasible. The surface photosynthetically available radiation was provided by monthly mean SeaWiFS products, and the monthly surface iron dust was from a model[44]. These latter two fields were climatological means and did not change in the simulations described here. Although the impact of changes in light and dust are likely to be important in the future, they are beyond the scope of this paper.

From the quasi-equilibrium state we conducted a range of different experiments (only experiments 2, 3 and 4 are discussed in the main text), where the system then adjusted under (some combination of) anthropogenic-induced drivers from 1860 to 2100.

Experiment 1 CONTROL. For another 240 years, the pre-industrial fields were used. This experiment provided a measure of the biogeochemical/ecological drift, and a baseline from which to compare the climate change experiments.

Experiment 2 ALL. The temperature, circulation, mixing and sea-ice fields and p_{CO_2} changed as predicted by the earth system model from 1860 to 2100. An ensemble of simulations were conducted with different randomization of the p_{CO_2} response function.

Experiment 3 p_{CO_2}-ONLY. The p_{CO_2} fields that affect biological rates were allowed to change from 1860 to 2100, but the circulation, mixing and sea-ice fields remained as for pre-industrial. An ensemble of simulations were conducted with different randomization of the p_{CO_2} response function.

Experiment 4 ALL-OTHER. p_{CO_2} fields were kept at pre-industrial conditions, while all other fields (temperature that affect biological rates, circulation, mixing and sea-ice) changed as though for 1860–2100.

Experiment 5 TEMP-ONLY. Temperature fields that affect biological rates changed from 1860–2100, but the circulation, mixing, sea-ice and p_{CO_2} fields remained as for pre-industrial conditions.

Experiment 6 PHYS-ONLY. Temperature fields remained as for pre-industrial conditions, but circulation, mixing fields, sea-ice and p_{CO_2} fields were allowed to change as for 1860–2100 conditions.

Note that these are independent experiments, with their own internal feedbacks. Thus it is not a priori given that, for instance, results from ALL-OTHER and p_{CO_2}-ONLY should add up to produce the results of ALL. When they do, it is useful to be able to see the independent effects of different environmental change drivers.

We also conduct several further sets of experiments to test the sensitivity of the results to different assumptions of the growth functions. In each of the below we performed the analogous experiments to one member of the ensemble of p_{CO_2}-ONLY and ALL:

Experiment a p_{CO_2}-MICHAELISMENTEN. In this experiment a more complex Michaelis–Menten p_{CO_2} growth function was assumed (Supplementary Fig. 2b):

$$\begin{aligned}
\gamma_j^{pCO_2} &= 1 \quad \text{if } p_{CO_2} < 400 \\
\gamma_j^{pCO_2} &= \min\left(1+\varepsilon_1\delta_j\frac{(p_{CO_2}-400)}{(p_{CO_2}-400)+k_{p_{CO_2}}}, 1+\delta_j\right) \\
&\quad \text{if } p_{CO_2} > 400, \delta_j > 0 \\
\gamma_j^{pCO_2} &= \max\left(1+\varepsilon_1\delta_j\frac{(p_{CO_2}-400)}{(p_{CO_2}-400)+k_{p_{CO_2}}}, 1+\delta_j\right) \\
&\quad \text{if } p_{CO_2} > 400, \delta_j < 0
\end{aligned} \tag{3}$$

This Michaelis–Menten type function requires two additional parameters (ε_1 and $k_{p_{CO_2}}$), which were set to 1.3 (unitless) and 150 µatm respectively.

Experiment b p_{CO_2}-HILL. In contrast to p_{CO_2}-MICHAELISMENTEN we assume a p_{CO_2} growth function that has slower response at lower p_{CO_2} and faster at high p_{CO_2} (Supplementary Fig. 2c):

$$\begin{aligned}
\gamma_j^{pCO_2} &= 1 \quad \text{if } p_{CO_2} < 400 \\
\gamma_j^{pCO_2} &= \min\left(1+\varepsilon_2\delta_j\frac{(p_{CO_2}-400)^2}{(p_{CO_2}-400)^2+k_{p_{CO_2}}{}^2}, 1+\delta_j\right) \\
&\quad \text{if } p_{CO_2} > 400, \delta_j > 0 \\
\gamma_j^{pCO_2} &= \max\left(1+\varepsilon_2\delta_j\frac{(p_{CO_2}-400)^2}{(p_{CO_2}-400)^2+k_{p_{CO_2}}{}^2}, 1+\delta_j\right) \\
&\quad \text{if } p_{CO_2} > 400, \delta_j < 0
\end{aligned} \tag{4}$$

Again this function requires two additional parameters (ε_2 and $k_{p_{CO_2}}$), which were set to 450 (unitless) and 12.25 µatm respectively.

These two functions (equations (3) and (4)) are the same as the original function (equation (2)) below 400 µatm and above 1,000 µatm, but differ in the speed of response to p_{CO_2}. Note that these function are not based on observations, but merely chosen to explore the sensitivity of the linear assumption in equation (2). Results suggest that the specific function alters the timing of, but not the final response (Supplementary Fig. 12).

Experiment c SPECIES48. Here only eight types were assumed within each functional group. Each type had the same temperature range as in the previous experiments (equation (1); Supplementary Fig. 1b). The original linear p_{CO_2} function (equation (2), Supplementary Fig. 2a) was assumed. We also conducted a CONTROL simulation for this series of experiments.

Experiment d SPECIES6. To explore the role of the genetic diversity that was imposed with the 16 (or 8) types within each functional group, here there was only one 'type' in each functional group. The types were no longer assumed to have temperature ranges, but instead to have a temperature growth function that spans the full range at the maximum value, as in the previous experiments (Supplementary Fig. 1c):

$$\gamma_j^T = \tau_T \exp\left(A_T\left(\frac{1}{T}-\frac{1}{T_N}\right)\right)$$

The p_{CO_2} function for each was assumed to be linear as in equation (2) with δ set by the mean GRR of the functional group. We also conducted a CONTROL experiment for this series of experiments.

Results from the experiments 5, 6 and a–d are not discussed in the main text, but are discussed in Supplementary Section S4 (Supplementary Figs 11–13).

Diagnostics. For describing the biogeography we calculated the region for each phytoplankton type where biomass was above a threshold value. We then defined the poleward (leading) edge and equatorward (trailing) edge of that region for each longitude for each hemisphere. Where a habitat spanned the equator there was no trailing edge. We also calculated the maximum of the biomass of each phytoplankton type for each longitude and each hemisphere. The results presented in Fig. 4b and Supplementary Figs 11c, 12c and 13c show the movement of the leading edge relative to pre-industrial averaged across longitude, types and hemispheres. We found similar changes to both the leading and trailing edges, as well as the maximum.

Two metrics of community structure were considered: 'genetic diversity' refers to the local assemblage of all 96 phytoplankton types, and 'functional diversity' refers to the local assemblage of the summed biomass of members of the six functional groups. We discuss only the latter in the main text. We calculated the genetic community structure ('genetic diversity') changes following Dutkiewicz *et al.*[5] as:

$$C_{gr}(t) = \sum_j^J \min\left(\frac{B_j(t)}{\sum_j^J B_j(t_o)}, \frac{B_j(t_o)}{\sum_j^J B_j(t_o)}\right)$$

where B_j was the biomass of each phytoplankton type, $J=96$ and t_o indicated pre-industrial biomass. If the community had not changed at all at time t, then $C_{gr}(t)=1$. If any (or all) phytoplankton types increased and none decreased, then $C_{gr}(t)$ was still 1: the original community was still there, but there was additional biomass. But if any phytoplankton types had decreased biomass, then $C_{gr}(t)<1$. We similarly defined functional community changes (fraction remaining) as:

$$C_{fr}(t) = \sum_k^K \min\left(\frac{F_k(t)}{\sum_k^K F_k(t_o)}, \frac{F_k(t_o)}{\sum_k^K F_k(t_o)}\right)$$

where F_k was the biomass of each functional group (that is, summation of biomass of all 16 types within each functional group), $K=6$.

We also calculated the amount of new community coming into a location:

$$C_{gn}(t) = \sum_{j}^{J} \min\left(\frac{B_j(t_o)}{\sum_j^J B_j(t)}, \frac{B_j(t)}{\sum_j^J B_j(t)}\right)$$

and similarly for $C_{fn}(t)$.

We note the genetic diversity changes are dependent on the parameterization of the genetic differences (see Supplementary Section 4). However, we find this metric useful to indicate how functional diversity can be maintained even while the genetic types can be significantly altered, and show this metric in the Supplementary Methods (Supplementary Figs 11b, 12b and 13b).

References

31. Marshall, J., Adcroft, A., Hill, C. N., Perelman, L. & Heisey, C. A finite-volume, incompressible Navier–Stokes model for studies of the ocean on parallel computers. *J. Geophys. Res.* **102,** 5753–5766 (1997).
32. Large, W. G., McWilliams, J. C. & Doney, S. C. Oceanic vertical mixing: A review and a model with a nonlocal boundary layer parameterization. *Rev. Geophys.* **32,** 363–403 (1994).
33. Gent, P. R. & McWilliams, J. C. Isopycnal mixing in ocean circulation models. *J. Phys. Oceanogr.* **20,** 150–155 (1990).
34. Sokolov, A. & Stone, P. H. A flexible climate model for use in integrated assessments. *Clim. Dynam.* **14,** 291–303 (1998).
35. Schlosser, C. A., Kicklighter, D. & Sokolov, A. *A Global Land System Framework for Integrated Climate-Change Assessments* Report No. 147 (MIT Joint Program for the Science and Policy of Global Change, 2007); http://web.mit.edu/globalchange/www/MITJPSPGC_Rpt147.pdf
36. Bonan, G. B. *et al.* The land surface climatology of the Community Land Model coupled to the NCAR Community Climate Model. *J. Clim.* **15,** 3123–3149 (2002).
37. Felzer, B. *et al.* Effects of ozone on net primary production and carbon sequestration in the conterminous United States using a biogeochemistry model. *Tellus B* **56,** 230–248 (2004).
38. Liu, Y. *Modeling the Emissions of Nitrous Oxide* (N_2O) *and Methane* (CH_4) *from the Terrestrial Biosphere to the Atmosphere* Report No. 10 (MIT Joint Program on the Science and Policy of Global Change, 1996); http://globalchange.mit.edu/files/document/MITJPSPGC_Report10.pdf
39. Kalnay, E. *et al.* The NCEP/NCAR 40-year reanalysis project. *Bull. Amer. Meteorol. Soc.* **77,** 437–470 (1996).
40. Randall, D. A. *et al.* in *Climate Change 2007: The Physical Science Basis* (eds Solomon, S. *et al.*) Ch. 8 (IPCC, Cambridge Univ. Press, 2007).
41. Yin, J. A consistent poleward shift of the storm tracks in simulations of 21st century climate. *Geophys. Res. Lett.* **32,** L18701 (2005).
42. Fyfe, J. C. & Saenko, O. A. Simulated changes in the extratropical Southern Hemisphere winds and currents. *Geophys. Res. Lett.* **33,** L06701 (2006).
43. Parekh, P., Follows, M. J. & Boyle, E. A. Decoupling of iron and phosphate in the global ocean. *Glob. Biogeochem. Cycles* **19,** GB2020 (2005).
44. Luo, C. *et al.* Combustion iron distribution and deposition. *Glob. Biogeochem. Cycles* **22,** GB1012 (2008).
45. Elrod, V. A., Berelson, W. M., Coale, K. H. & Johnson, K. S. The flux of iron from continental shelf sediments: A missing source for global budgets. *Geophys. Res. Lett.* **31,** L12307 (2004).
46. Follows, M. J., Dutkiewicz, S., Grant, S. & Chisholm, S. W. Emergent biogeography of microbial communities in a model ocean. *Science* **315,** 1843–1846 (2007).
47. Dutkiewicz, S., Follows, M. J. & Bragg, J. Modeling the coupling of ocean ecology and biogeochemistry. *Glob. Biogeochem. Cycles* **23,** GB1012 (2009).
48. Kooijman, S. A. L. M. *Dynamic Energy and Mass Budget in Biological Systems* (Cambridge Univ. Press, 2000).
49. Bissinger, J. E., Montagnes, D. J. S., Sharples, J. & Atkinson, D. Predicting marine phytoplankton maximum growth rates from temperature: Improving on the Eppley curve using quantile regression. *Limnol. Oceanogr.* **53,** 487–493 (2008).